Preparation and Characterization of L-[5-^{11}C]-Glutamine for Metabolic Imaging of Tumors

Wenchao Qu[1], Shunichi Oya[1], Brian P. Lieberman[1], Karl Ploessl[1], Limin Wang[1], David R. Wise[2], Chaitanya R. Divgi[1], Lewis P. Chodosh[2], Craig B. Thompson[2], and Hank F. Kung[1]

[1]*Departments of Radiology and Pharmacology, University of Pennsylvania, Philadelphia, Pennsylvania; and* [2]*Department of Cancer Biology, Abramson Cancer Center, University of Pennsylvania, Philadelphia, Pennsylvania*

Recently, there has been a renewed interest in the study of tumor metabolism above and beyond the Warburg effect. Studies on cancer cell metabolism have provided evidence that tumor-specific activation of signaling pathways, such as the upregulation of the oncogene *myc,* can regulate glutamine uptake and its metabolism through glutaminolysis to provide the cancer cell with a replacement of energy source. **Methods:** We report a convenient procedure to prepare L-[5-^{11}C]-glutamine. The tracer was evaluated in 9L and SF188 tumor cells (glioma and astrocytoma cell lines). The biodistribution of L-[5-^{11}C]-glutamine in rodent tumor models was investigated by dissection and PET. **Results:** By reacting ^{11}C-cyanide ion with protected 4-iodo-2-amino-butanoic ester, the key intermediate was obtained in good yield. After hydrolysis with trifluoroacetic and sulfonic acids, the desired optically pure L-[5-^{11}C]-glutamine was obtained (radiochemical yield, 5% at the end of synthesis; radiochemical purity, >95%). Tumor cell uptake studies showed maximum uptake of L-[5-^{11}C]-glutamine reached 17.9% and 22.5% per 100 μg of protein, respectively, at 60 min in 9L and SF188 tumor cells. At 30 min after incubation, more than 30% of the activity appeared to be incorporated into cellular protein. Biodistribution in normal mice showed that L-[5-^{11}C]-glutamine had significant pancreas uptake (7.37 percentage injected dose per gram at 15 min), most likely due to the exocrine function and high protein turnover within the pancreas. Heart uptake was rapid, and there was 3.34 percentage injected dose per gram remaining at 60 min after injection. Dynamic small-animal PET studies in rats bearing xenografted 9L tumors and in transgenic mice bearing spontaneous mammary gland tumors showed a prominent tumor uptake and retention. **Conclusion:** The data demonstrated that this tracer was favorably taken up in the tumor models. The results suggest that L-[5-^{11}C]-glutamine might be useful for probing in vivo tumor metabolism in glutaminolytic tumors.

Key Words: PET imaging; tumor metabolism; ^{18}F-FDG; gene expression; *myc*

J Nucl Med 2012; 53:98–105
DOI: 10.2967/jnumed.111.093831

Even in environments with a plentiful oxygen supply, tumor cells tend to derive energy from glycolysis, thereby leading to an overproduction of lactic acid. Warburg first observed this effect, a process that now bears his name (*1–8*). The increase of glucose utilization in tumor cells is due, in part, to PI3K/Akt/mTOR-mediated upregulation of glucose transporters and hexokinase 2, which enzymatically phosphorylates and traps glucose inside the cell. This is the biochemical basis of using ^{18}F-FDG PET as a diagnostic tool for the detection of human cancers (*9,10*). Despite the utility of ^{18}F-FDG PET for staging and monitoring of cancer in humans, there is a growing realization that up to 30% of actively growing cancers are ^{18}F-FDG–negative and cannot be detected by ^{18}F-FDG PET (*11*). The observation strongly suggests that tumor cells may have alternative nutrient and metabolic strategies for survival and that glucose may not be the only source of energy and metabolic substrates for tumor growth (Fig. 1). Consequently, developing new metabolic probes for ^{18}F-FDG–negative tumors is an understudied yet critical endeavor for advancing the field of cancer diagnosis and developing new cancer therapeutics.

Since the 1950s, glutamine has been recognized as an important tumor nutrient that contributes to key metabolic processes in proliferating cancer cells (*12*). Glutamine participates in bioenergetics, supports cell defenses against oxidative stress, complements glucose metabolism, and is an obligate nitrogen donor for nucleotide and amino acid synthesis (*4,6,13*). To date, the only oncogene known to influence glutamine uptake and metabolism is *myc,* which has been shown to induce glutamine addiction in certain cancer cell lines in vitro (*13,14*). Specifically, *myc* can render tumor cells dependent on glutamine uptake for viability by directly regulating the levels of the glutamine transporter slc1a5 and indirectly regulating glutaminase expression through miR-23a/b (*13–17*). Glutaminase is a key enzyme that converts glutamine to glutamate and whose expression has been previously shown to be required for tumor growth (Fig. 1) (*18,19*). The rationale for using labeled glutamine and its related derivatives is evident. But, it is likely that using L-[5-^{11}C]-glutamine PET to study glutaminolysis might measure the additive effects of upregulation of glu-

Received May 27, 2011; revision accepted Aug. 17, 2011.
For correspondence or reprints contact: Hank F. Kung, Departments of Radiology and Pharmacology, University of Pennsylvania, 3700 Market St., Philadelphia, PA 19104.
E-mail: kunghf@sunmac.spect.upenn.edu
Published online Dec. 15, 2011.

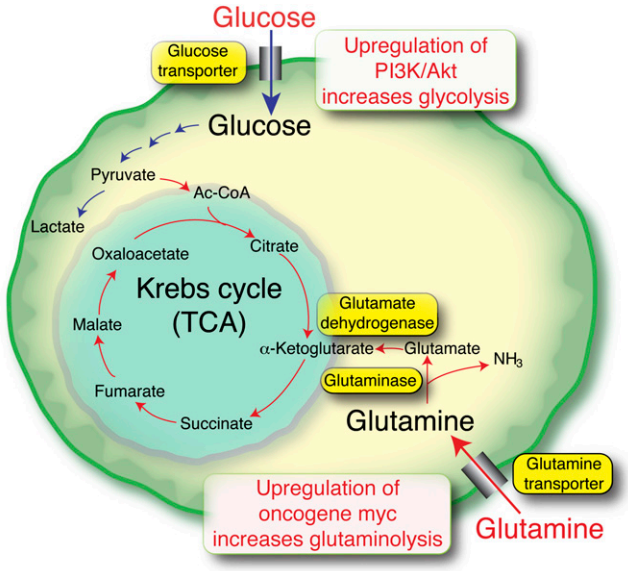

FIGURE 1. Simplified schematic drawing of intracellular metabolism of glucose and glutamine is presented to show possible metabolic changes in tumor cells using glycolysis or glutaminolysis. Tumor cells may use both pathways to generate energy and intermediate metabolites for survival and growth. However, tumor cells may switch energy source to glutamine and, thus, enhance their survival and proliferation. Ac-CoA = acetyl-coenzyme A.

tamine transport and glutamine use. Similar to the tumor cell trapping of ^{18}F-FDG through upregulation of membrane-bound glucose transporter 1 and cytosol hexokinase, glutamine may be used via the glutamine transporter (ASCT2) and glutaminases located in the cytosol (*9,11,18*). Previously, ^{13}N-glutamine imaging of various spontaneous canine tumors showed that the imaging agent displayed a positive correlation with postmortem findings (*20*).

In this report, we demonstrate that L-[5-^{11}C]-glutamine can be prepared by an ^{11}C-cyanide nucleophilic reaction. A successive 1-pot high-strength acid deprotection and controlled hydrolysis reaction formed optically pure L-[5-^{11}C]-glutamine in good radiochemical yield. The glutamine uptake was assessed in tumor cells and 9L and SF188 tumor cells (glioma and astrocytoma cell lines). In vivo metabolism related to glutaminolysis in tumor tissues was evaluated by PET of rodent tumor models.

MATERIALS AND METHODS

^{1}H nuclear magnetic resonance (NMR) spectra were recorded on a DPX 200 spectrometer (Bruker). High-resolution mass spectroscopy was performed on an LC/MSD time-of-flight mass spectrometer (Agilent). Solvent dimethyformamide was purified by a PureSolv (Innovative Technology Inc.) solvent purification system immediately before use. All other chemicals were purchased from Aldrich Chemical Co. and used without further purification. ^{11}C-CO_2 was produced by the ^{14}N(p,α)^{11}C nuclear reaction with an IBA cyclone 18/9 or JSW 3015 cyclotron at the cyclotron facility (University of Pennsylvania). High-performance liquid chromatography (HPLC) measurements were run on an Agilent1200/1100 HPLC series with variable-wavelength ultraviolet detector and γ-detector.

(S)-*Tert*-Butyl 2-((*Tert*-Butoxycarbonyl) Amino)-4-(Tosyloxy)Butanoate

To a solution of alcohol (**1**) (0.9 g, 3.25 mmol, reported previously (*21*)), *p*-toluenesulphonyl chloride (1.24 g, 6.5 mmol), and triethylamine (1.6 g, 15.6 mmol) in anhydrous dichloromethane (15 mL) was added dimethylaminopyridine (0.039 g, 0.32 mmol) at 0°C. The mixture was stirred at room temperature for 3 h, ice (5 g) was added, and the mixture was extracted with dichloromethane. The organic layer was dried, and solvent was removed in vacuo. The crude mixture was purified by flash column (silica gel) chromatography (hexanes/ethyl acetate 10/0 to 6/4, R_f = 0.4, hexanes/ethylacetate 6/4) to yield (*S*)-*tert*-butyl 2-((*tert*-butoxycarbonyl)amino)-4-(tosyloxy)butanoate (**2**) as a colorless oil (1.08 g, 77%). During storage in the freezer, it gradually converted to a pale white solid, melting point 60–62°C, $[\alpha]_D^{25} = -16.8$ (c = 1, MeOH); ^{1}H NMR ($CDCl_3$): δ 7.76 (d, *J* = 8.0 Hz, 2H), 7.32 (d, *J* = 8.0 Hz, 2H), 4.9 (br s, N*H*), 4.14 (m, 1H), 4.08 (t, *J* = 6.0 Hz, 2H), 2.42 (s, 3H), 2.0–2.2 (m, 2H), 1.41 (s, 9H), 1.38 (s, 9H): high-resolution mass spectroscopy calculated for $C_{20}H_{32}NO_7S$ $[M + H]^+$, 430.1899; observed, 430.1897.

(S)-*Tert*-Butyl 2-((*Tert*-Butoxycarbonyl) Amino)-4-Iodobutanoate

The solution of **2** (250 mg, 0.58 mmol) in anhydrous acetone (5 mL) was stirred with NaI (174 mg, 1.16 mmol) for 3 h at 60°C. Solid residue was removed by filtration. The filtrate was concentrated at reduced pressure, and the residue was purified by flash column (silica gel) chromatography (hexanes, ethyl acetate; 5:1; R_f = 0.6) to yield (*S*)-*tert*-butyl 2-((*tert*-butoxycarbonyl)amino)-4-iodobutanoate (**3**) as a pale yellow solid (0.182 g, 81%), melting point, 44–46°C, $[\alpha]_D^{25} = -31.4$ (c = 1.02, MeOH); ^{1}H NMR ($CDCl_3$): δ 5.1 (br s, N*H*), 4.3 (m, 1H), 3.2 (t, *J* = 6.0 Hz, 2H), 2.1–2.4 (m, 2H), 1.50 (s, 9H), 1.47 (s, 9H): high-resolution mass spectroscopy calculated for $C_{13}H_{25}INO_3$ $[M + H]^+$ 408.0648; observed, 408.0648.

L-[5-^{11}C]-Glutamine

^{11}C-CO_2 produced by cyclotron was converted to ^{11}C-HCN using a custom-made reaction module. Briefly, ^{11}C-CO_2 was converted to ^{11}C-CH_4 with a hydrogen and nickel catalyst at 360°C. ^{11}C-CH_4 was passed across the Oxisorb (Sigma-Aldrich Inc.) cartridge with argon carrier gas to remove moisture, oxygen, and unreacted ^{11}C-CO_2. Resulting ^{11}C-CH_4 gas was mixed with anhydrous ammonia gas and directed to a platinum wire–packed quartz tube placed in the furnace at 1,000°C. The ^{11}C-HCN gas generated was trapped in the KOH solution of dimethyformamide in a reaction vial for the next reaction. To the solution of ^{11}C-HCN in dimethyformamide/KOH (300 μL/1 mg) was added the solution of **3** (4 mg) in dimethyformamide (300 μL). The mixture was heated for 5 min at 120°C. After cooling to room temperature, water (10 mL) was added, and the mixture was passed through a C-18 Plus (Waters) cartridge. The cartridge was further washed with water (2 × 10 mL). The intermediate product, 5-^{11}C-(*S*)-*tert*-butyl 2-((*tert*-butoxycarbonyl)amino)-4-cyanobutanoate (**4**), which was trapped on the cartridge, was eluted with acetonitrile (2 mL). Solvent was removed under a vacuum with gentle nitrogen bubbling and external heating (120°C). Excess acetonitrile (1 mL) was added to aid in the removal of residual water azeotropically.

To the dried residue of **4**, trifluoroacetic acid/H_2SO_4 (4/1 ratio, 0.5 mL) was added, and the solution was heated at 120°C for 10 min. After cooling to room temperature, Na_2CO_3 (aqueous saturated) solution (2 mL) was carefully added, and the mixture was passed through a C18 light (Waters) cartridge. The eluent was further passed through a short column of Ag11-A8 resin (4 g; Bio-Rad). The column was washed with excess water (3 mL) to recover the activity. L-[5-^{11}C]-glutamine (**5**) was obtained as a clear solution in water (6 mL, pH 7). The solution was applied to biologic study without further purifications. The whole procedure required approximately 60 min, with 1.85–2.59 GBq of **5** obtained from approximately 55.5 GBq of ^{11}C-CO_2. Radiochemical yield was 25%–40% (decay-corrected). Radiochemical purity and optical purity were determined by chiral HPLC (Chirex 3216 column [Phenomenex], 1 mM $CuSO_4$, 1 mL/min, ultraviolet 254-nm and γ-detector). Radiochemical purity was greater than 94%. Optical purity was 95% ± 5% (n = 5). The same HPLC conditions were used to estimate the specific activity of **5** using a standard cold solution of L-glutamine. Specific activity was 1.85 ± 0.74 GBq/μmol at the end of synthesis (n = 5).

Cell Culture

Tumor cells, 9L cells (American Type Culture Collection), and SF188 cells (Neurosurgery Tissue Core, University of California) were cultured in Dulbecco modified Eagle medium (Gibco BRL) supplemented with 10% fetal bovine serum (Hycolne) and 1% penicillin and streptomycin. In addition, 1% L-glutamine was added in medium for $SF188_{bcl\text{-}xl}$ cells. Cells were maintained in a T-75 culture flask under humidified incubator conditions (37°C, 5% CO_2) and were routinely passaged at confluence.

Cell Uptake Studies

Tumor cells were plated in culturing medium 24 h before studies. On the day of the experiment, the medium was aspirated and the cells were washed 3 times with phosphate-buffered saline (PBS; containing Ca^{2+} and Mg^{2+}). L-[5-^{11}C]-glutamine and L-[3,4-^{3}H(N)]-glutamine were mixed in PBS (with Ca^{2+} and Mg^{2+}) solution and were then added to each well (148 kBq of L-[5-^{11}C]-glutamine and 37 kBq of ^{3}H-L-glutamine per well). ^{3}H-L-glutamine, which was purchased from Perkin Elmer with more than 97% radiochemical purity and a specific activity of 1.11–2.22 TBq/mmol, was used as a reference compound. The cells were incubated at 37°C for 5, 15, 30, and 60 min. At the end of the incubation period, the PBS solution containing both tracers was aspirated, and then the cells were washed 3 times with 1 mL of ice-cold PBS without Ca^{2+} and Mg^{2+}. After being washed with ice-cold PBS, 350 μL of 0.1N NaOH was used to lyse the cells. The lysed cells were collected onto filter paper and counted together with samples of the initial dose using a γ-counter (Packard Cobra). After 24 h, ^{3}H activity was counted using a scintillation counter (LS 6500; Beckman). The cell lysate (200 μL) was used for determination of protein concentration by modified Lowry protein assay. The data were normalized as percentage uptake of initial dose relative to 100 μg of protein content (%ID/100 μg of protein).

In Vitro Protein Incorporation

To measure the extent of protein incorporation of L-[5-^{11}C]-glutamine protein-bound activity in SF188 and 9L cells was determined 30 min after incubation. The cells were incubated with 1,184 kBq of L-[5-^{11}C]-glutamine and 37 kBq of ^{3}H-L-glutamine (purchased from Perkin Elmer/NEN) as the internal reference, in 3 mL of PBS. At the end of incubation, radioactive medium was removed, and the cells were washed 3 times with ice-cold PBS without Ca^{2+} and Mg^{2+} and treated with 0.25% trypsin and resuspended in PBS. The samples were centrifuged (18,000g, 5 min), the supernatant was removed, and the cells were suspended in 200 μL of 1% Triton-X 100 (Sigma). After stirring in a vortex mixer, 800 μL of ice-cold 15% trichloroacetic acid (TCA) were added to the solution. After a 30-min precipitation, the cells were centrifuged again (18,000g, 15 min) and washed twice with 15% ice-cold TCA. The radioactivity in both supernatant and pellet was determined. Protein incorporation was calculated as percentage of acid-precipitable activity.

In Vivo Biodistribution Study in Imprinting Control Region (ICR) Mice

To test L-[5-^{11}C]-glutamine as a tumor PET agent, we first evaluated in vivo biodistribution of this tracer in normal ICR mice (20–25 g, 3 mice per group). The mice were anesthetized under isoflurane (2%–3%), and 0.15 mL of saline solution containing 30 MBq of L-[5-^{11}C]-glutamine was injected via the lateral tail vein. The mice were sacrificed at 15, 30, and 60 min after injection by cardiac excision while under isoflurane anesthesia. The organs of interest were removed and weighed, and the radioactivity was counted with a γ-counter (Packard Cobra). The percentage dose per gram was calculated by a comparison of the tissue activity counts to counts of 1% of the initial dose. The initial dose consisted of 100 times diluted aliquots of the injected material measured at the same rate (0.5 min/sample, 80% efficiency).

Small-Animal PET

Dynamic small-animal PET studies were conducted with L-[5-^{11}C]-glutamine. All scans were obtained on a dedicated small-animal PET scanner (Mosaic; Phillips) that had a field of view of 11.5 cm (*22*). F344 rats with 9L xenografts and transgenic mice bearing M/tomND spontaneous human mammary tumors were used for the imaging studies. All animals were subjected to isoflurane anesthesia (2%–3%, 1 liter of oxygen per minute) and were then placed on a heating pad to maintain body temperature throughout the procedure. Animals were visually monitored for breathing and any other signs of distress throughout the entire imaging period. F344 rats were injected with 66.2 MBq of L-[5-^{11}C]-glutamine and transgenic mice were injected with 21.1 MBq of L-[5-^{11}C]-glutamine respectively. Data acquisition began after an intravenous injection of the tracer. All scans were obtained over a period of 60 min (dynamic, 5 min/frame). The frames were analyzed and reconstructed with Amide's a Medical Imaging Data Examiner analysis software.

RESULTS

Chemistry and Radiochemistry

The synthesis of L-[5-11C]-glutamine was performed as follows (Scheme 1): the partially protected homoserine was converted to tosylate by a treatment of tosyl chloride, triethylamine at room temperature (*21*). A Finkelstein reaction smoothly provided radiolabeling of the iodide precursor, with satisfied yield. Although tosylate could be directly used as a precursor for radiolabeling, it was found that iodide consistently provided higher radiolabeling yields. The radiolabeling process started with the conversion of ^{11}C-CO_2 to ^{11}C-cyanide ion according to a previously

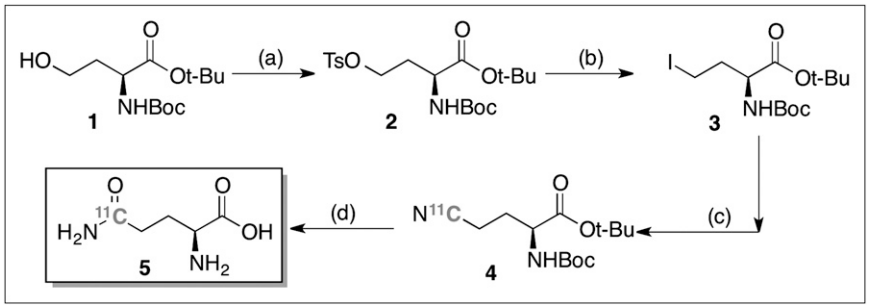

SCHEME 1. Scheme for synthesis of precursor and radiolabeling of L-[5-^{11}C]-glutamine. Reagents and conditions: (a) p-Toluenesulfonylchloride, triethylamine, dimethylaminopyridine, DCM, r.t.; (b) KI, acetone, reflux; (c) K^{11}CN, dimethyformamide, KOH, 5 min, 120°C; and (d) trifluoroacetic acid/H_2SO_4, 10 min, 120°C. 1 = homoserine; 2 = tosylate; 3 = iodide; 4 = 11C-cyanoderivative; 5 = L-[5-^{11}C]-glutamine.

reported method (*23*). Briefly, ^{11}C-CO_2 was converted to ^{11}C-CH_4 with a hydrogen and nickel catalyst at 360°C. This ^{11}C-CH_4 gas was further mixed with anhydrous ammonia gas and directed to a platinum wire–packed quartz tube placed in the furnace at 1,000°C. The ^{11}C-HCN gas generated was trapped in the KOH solution of dimethyformamide in a reaction vial and formed the desired potassium cyanide (^{11}C-KCN). Next, the obtained ^{11}C-cyanide ion was reacted with the iodide precursor to produce an intermediate ^{11}C-cyanoderivative, which was treated with a trifluoroacetic acid/H_2SO_4 mixture for hydrolysis (*24*). The hydrolysis produced only glutamine, with more than 94% radiochemical purity, and no detectable amount of glutamic acid. In addition, the optical purity of the product was also measured with chiral HPLC and the result revealed that the amount of L-glutamine in the final product was higher than 95% (Fig. 2). After neutralization and treatment with ion retardation Ag11-A8 resin, more than 1.85 GBq of L-[5-^{11}C]-glutamine (~25% radiochemical yield) was produced in 60 min. This method is more efficient than the previously reported enzymatic preparation (*25*).

In Vitro Cell Uptake Studies

Time-dependent uptake of L-[5-^{11}C]-glutamine in PBS was determined in rat glioma 9L and human glioblastoma SF188 cells (Fig. 3). L-[5-^{11}C]-glutamine demonstrated high uptake and linear incremental uptake within 60 min in both cell lines. Uptake in the SF188 cell line, which has shown a 25-fold amplification of the oncogene *myc,* was higher than that in 9L cells. The maximum uptake of L-[5-^{11}C]-glutamine reached 17.9% and 22.5% uptake/100 μg of protein at 60 min in 9L and SF188 cells, respectively. In the dual-isotope studies, uptake of ^{3}H-L-glutamine was similar to that of L-[5-^{11}C]-glutamine under the same condition (e.g., ^{3}H-L-glutamine had 13.5% uptake/100 μg of protein at 30 min in SF188 cells, which was comparable to 15.6% uptake/100 μg protein for L-[5-^{11}C]-glutamine). A comparable experiment using ^{3}H-L-glutamic acid showed one tenth of the cell uptake (1%–2% uptake/100 μg protein, data not shown).

In Vitro Protein Incorporation

Incorporation of L-[5-^{11}C]-glutamine into protein in 9L and SF188 cell lines was measured at 30 min after incubation (Table 1). In this dual-isotope experiment ^{3}H-L-glutamine was used as a reference compound. As expected, L-[5-^{11}C]-glutamine and ^{3}H-L-glutamine incorporated with comparable values into protein as measured by the trichloroacetic acid precipitation method; the percentage incorporation in the 9L cells was 44.1% ± 2.28% and 53.7% ± 3.18%, respectively, whereas the protein incorporation in the SF188 tumor cells was 26.7 ± 0.48 and 35.5% ± 2.77%, respectively. The results further suggest that the tumor cells promptly used L-glutamine as the source of energy, and it is likely that the L-glutamine was rapidly introduced inside the cytosol and incorporated into protein and other macromolecules.

In Vivo Biodistribution Study in ICR Mice

In vivo biodistribution studies were performed in male ICR mice (20–25 g) (Table 2). The distribution of L-[5-^{11}C]-glutamine showed the expected behavior of a radiolabeled amino acid with significant pancreas uptake (7.37% dose/g at 15 min), most likely due to the exocrine function and high protein turnover within the pancreas. Pancreatic function requires the use of various amino acids

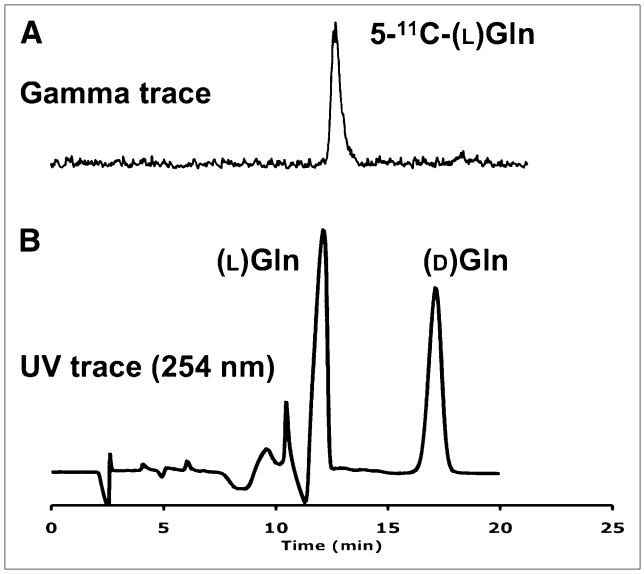

FIGURE 2. (A) HPLC profile (γ-trace) of L-[5-^{11}C]-glutamine. (B) Ultraviolet (UV) profiles of cold L-glutamine and D-glutamine at 254 nm. γ-trace shows that radiochemical purity is >99%. Optical purity, L-to-D ratio, was >95% (Chirex 3126 (D)-penicillamine 250 × 4.6 mm column; mobile phase: 2 mM $CuSO_4$, 1 mL/min [Phenomenex]).

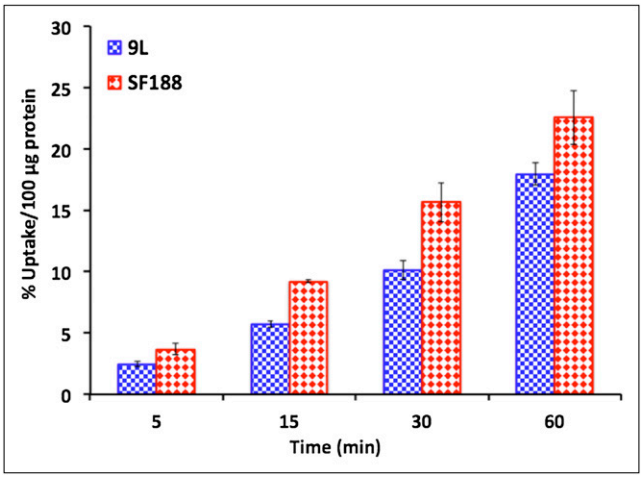

FIGURE 3. Uptake of L-[5-^{11}C]-glutamine in 9L and SF188 glioma cell lines. Data are mean ± SD, $n = 3$.

as precursors for protein and peptide synthesis. Heart uptake and retention drop rapidly at 15 min after injection, showing lower activity at 60 min after injection (3.34% dose/g). Initial lung and kidney uptake was prominent but quickly washed out at 60 min after injection. Rapid uptake of the tracer is observed within the kidneys, but the tracer is quickly excreted through the urinary bladder. L-[5-^{11}C]-glutamine showed moderate liver uptake with a relatively slow washout rate. The brain exhibited moderate uptake of 1.49 %ID/g at 15 min after injection and rapidly washed out to 0.89 %ID/g at 60 min.

Small-Animal PET Studies in F344 Rats with 9L Xenografts and Transgenic Mouse with M/tomND Spontaneous Tumors

Dynamic small-animal PET studies for rats bearing 9L tumor xenografts and transgenic mice bearing spontaneous M/tomND tumors were performed with L-[5-^{11}C]-glutamine (Fig. 4). Animal PET images of summed 60-min coronal, transverse, and sagittal sections were selected for visualization. As the images demonstrate, clear tumor uptake is visualized within each animal model, despite the necrotic tissue observed within the F344 rat tumor. To confirm this finding, region-of-interest analysis was performed using Amide analysis software on the reconstructed images to generate the time–activity curves for L-[5-^{11}C]-glutamine.

TABLE 1
Protein Incorporation of L-[5-^{11}C]-Glutamine and ^{3}H-L-Glutamine in Glioma Cells After 30-Minute Incubation Period

Cells	Protein incorporation (%) of L-[5-^{11}C]-glutamine	Protein incorporation (%) of ^{3}H-L-glutamine
9L	44.1 ± 2.28	53.7 ± 3.18
SF188	26.7 ± 0.48	35.5 ± 2.77

Data are percentage incorporation of TCA-precipitated fraction, presented as mean ± SD ($n = 3$).

TABLE 2
Biodistribution of L-[5-^{11}C]-Glutamine in Normal Mice

Organ	15 min	30 min	60 min
Blood	1.56 ± 0.56	1.01 ± 0.04	0.92 ± 0.14
Heart	6.07 ± 0.65	3.49 ± 0.30	3.34 ± 0.45
Muscle	0.70 ± 0.01	0.68 ± 0.07	0.61 ± 0.15
Lung	5.39 ± 0.20	3.36 ± 0.54	2.39 ± 0.31
Kidney	5.34 ± 0.41	3.84 ± 0.30	3.54 ± 0.97
Pancreas	7.37 ± 0.44	7.06 ± 0.97	6.27 ± 0.62
Spleen	2.85 ± 0.02	1.79 ± 0.24	1.79 ± 0.31
Liver	3.99 ± 0.13	2.90 ± 0.26	2.67 ± 0.35
Skin	1.20 ± 0.18	0.93 ± 0.09	0.68 ± 0.03
Brain	1.49 ± 0.05	0.96 ± 0.06	0.89 ± 0.12

Data are %ID/g ± SD ($n = 3$).

The kinetics indeed confirm that the tracer exhibited higher tumor uptake than did the background (muscle) regions. The tumor uptake appeared consistent throughout the time period, suggesting an efficient trapping in the tumor.

Rapid tumor uptake is visualized within the m/tomND mouse model in the first 10–15 min (Fig. 5). At 15 min after injection, tumor washout is rapid through the 60-min scan time. Within the F344 animal model, maximum tumor uptake was reached within the first 20 min after injection. Tumor uptake then remained consistent throughout the 60-min scan time, with little to no washout observed, suggesting that the radioactivity was taken up and trapped in the tumor tissue. High liver, kidney, and bladder uptake was observed in both animal models. However, the activity in the tumor washed out. The kinetics of tumor retention are different from those observed for 9L tumor in rats.

DISCUSSION

Emerging evidence suggests that glutamine, which is the most abundant nonessential amino acid in the human body, may be an alternative nutrient for tumor growth (*6,18*). Glutamine is stored in skeletal muscle and circulates in blood at high concentration (0.5–1 mmol/L). Recently, it has become clear that glutaminolysis, which involves the mitochondrial catabolism of glutamine to lactate and CO_2, may provide alternate energetic and metabolic pathways for tumor cells to sustain growth. Consequently, cancer cells may become addicted to glutamine to support their energetic needs in much the same way as ^{18}F-FDG–positive cancers are thought to rely on glucose to meet their energetic demands (Fig. 1) (*1,9,26*). Importantly, aerobic glycolysis and glutaminolysis are not mutually exclusive and these processes may occur concomitantly in tumors. As such, it is likely that a dynamic balance between these 2 processes is an essential strategy for tumor cell survival. Nevertheless, the ability of some tumors to preferentially use glutamine rather than glucose to satisfy their metabolic needs suggests that ^{18}F-FDG PET–negative tumors may have elevated rates of glutaminolysis. The PI3K/Akt signal transduction pathway stimulates aerobic glycolysis in tu-

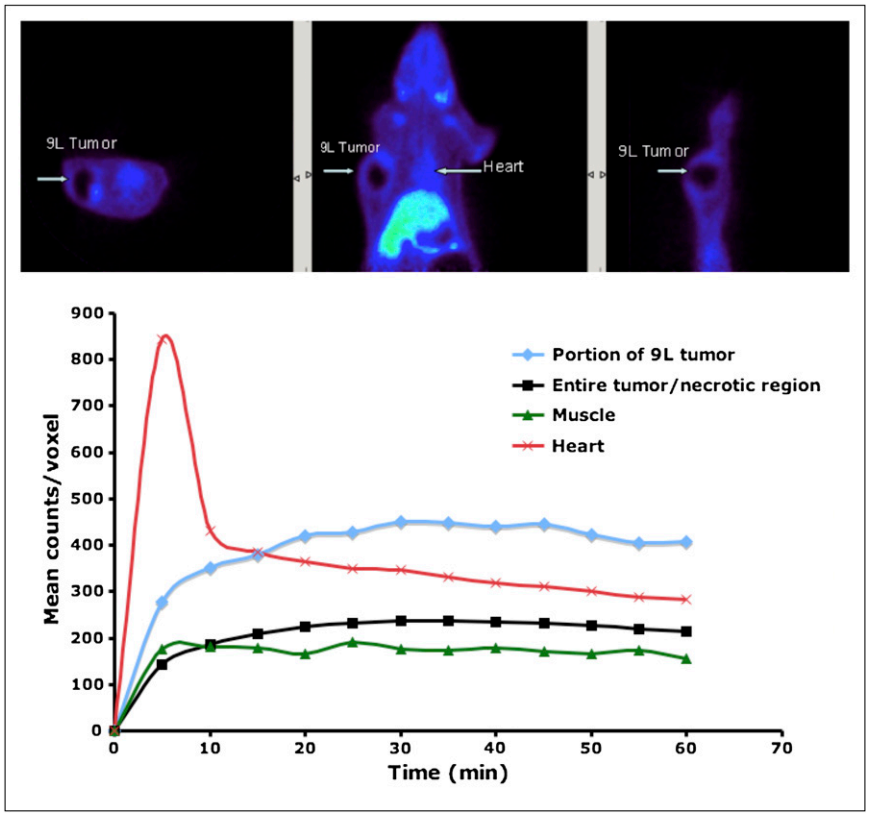

FIGURE 4. (Upper) small-animal PET images of L-[5-^{11}C]-glutamine in xenografted 9L tumor of F344 rat after intravenous injection. Data represent images from summed 60-min scan. Images are shown in transverse, coronal, and sagittal views. Note areas of necrosis within 9L tumor (donut shape). Arrows correspond to organs and tissues of interest. (Lower) small-animal PET time–activity curve for L-[5-^{11}C]-glutamine after intravenous injection into F344 rat. Xenografted 9L tumor was clearly visualized; however, there was necrotic tissue in middle of tumor, which does not show glutamine uptake (donut shape). Heart, liver, and pancreas uptake was also prominent, as is consistent with biodistribution data.

mor cells, thereby diverting the TCA cycle from oxidative phosphorylation to the production of metabolites for fatty acid and amino acid synthesis, which are required for cell proliferation. This is the major mechanism that enables ^{18}F-FDG PET of human cancers. In an analogous manner, activation of the oncogene *myc* has been reported to coordi-

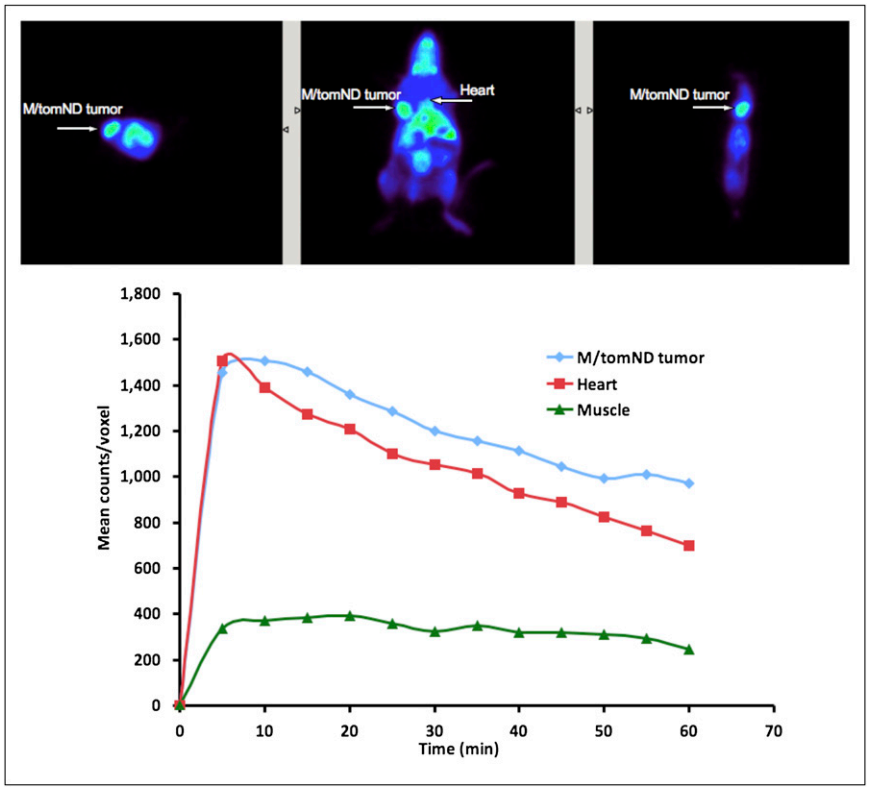

FIGURE 5. (Upper) small-animal PET images of L-[5-^{11}C]-glutamine in transgenic mouse bearing m/tomND tumor after intravenous injection. Data represent images from summed 60-min scan. Images are shown in transverse, coronal, and sagittal views. Arrows correspond to organs and tissues of interest. (Lower) small-animal PET time–activity curve for L-[5-^{11}C]-glutamine after intravenous injection into tumor-bearing transgenic mouse. Human mammary tumor showed high uptake, as compared with background (muscle). Heart uptake was also high, similar to biodistribution data in normal mice.

nate the expression of gene products necessary for cells to use glutamine as an energy source, rather than glucose. As such, *myc* activation drives glutaminolysis whereas the PI3K/Akt pathway drives aerobic glycolysis. These 2 processes may occur concomitantly in tumor cells, thereby conferring specific adaptive advantages for tumor growth. Therefore, labeled glutamine could potentially be useful to discriminate a tumor's reliance on different nutrients for growth.

Glutamine transporters play an important role in mammalian cell biology, and these include SNAT1, SNAT3, SNAT5, SLC6A19, and ASCT2 (*27,28*). Among these, ASCT2 appears to be the glutamine transporter most commonly used in actively growing tumors and ASCT2 is upregulated in tumor cells in a manner analogous to the upregulation of the glucose transporter, GLUT1, in tumors using aerobic glycolysis. Increased uptake of glutamine may result in enhanced accumulation of labeled glutamine tracers in tumors, thereby enabling their imaging. The competition experiment suggests that this mechanism, at least in part, is responsible for the tumor cell uptake.

Several ^{11}C- and ^{18}F-labeled amino acids have been used as PET tumor imaging agents in humans (*28*). These include L-^{11}C-methionine, L-^{18}F-fluoro-α-methyl-tyrosine, *O*-(2-^{18}F-fluoro-ethyl) tyrosine, and anti-1-amino-3-^{18}F-fluorocyclobutyl-carboxylic acid (FACBC) (*29–33*). Uptake of these tracers permits imaging of primary and metastatic tumors and is likely related to the increased expression of amino acid transporters in tumors. As such, PET with these tracers shows promise as a tool for the diagnosis and staging of human cancers. Anti-^{18}F-FACBC is a α, α-dialkyl nonmetabolizable amino acid. Uptake of anti-^{18}F-FACBC, which is an analog of leucine, is mediated by the sodium-independent L large-neutral amino acid transport system and to a lesser extent by ASCT2 (*34*). Recent human studies suggest that it is a potential imaging agent for prostate tumors (*32,33*). Compared with ^{18}F-FDG, anti-^{18}F-FACBC shows low renal excretion. Apparently, once it is transported across the membrane, no further metabolism occurs. Another labeled amino acid derivative, *O*-(2-^{18}F-fluoroethyl)-L-tyrosine, is a tyrosine analog that is transported across the cell membrane via L large-neutral amino acid transport system and is not incorporated into cellular proteins. In contrast to ^{18}F-FDG and methionine, it is not taken up in inflammatory cells. As such, it is often used for imaging brain tumors, such as gliomas (*35*). Incorporation of labeled amino acids into protein in vivo may not be a desirable characteristic for an imaging agent. However, at this moment we do not know how this imaging agent eventually would behave in humans. The mechanism of uptake of *O*-(2-^{18}F-fluoroethyl)-L-tyrosine appears to be related to the upregulation of amino acid transporters at the tumor cell membrane. All currently reported amino acid–based PET agents are designed to take advantage of the increase of amino acid transporters. However, because they are not structurally related to glutamine, they are unlikely to be specific for changes in glutaminolytic tumors.

Recently, a novel series of fluorinated glutamine has been reported (*21,36*). We reported a glutamine analog, ^{18}F-(*2S,4R*)4-fluoroglutamine, that also was selectively taken up and trapped by tumor cells (*21*). This new tracer, which has a longer physical half-life (110 min), may provide a more convenient and useful tool for mapping glutamine metabolism. In addition, we recently reported using specifically deuterated [5-^{13}C-4-$^{2}H_2$]-L-glutamine in conjunction with hyperpolarized magnetic resonance spectroscopy for studying glutaminolysis in proliferating tumor cells (*37*). The results of this hyperpolarized magnetic resonance spectroscopy experiment provided additional proof that SF188 tumor cells use glutamine as the energy source.

CONCLUSION

The new tracer L-[5-^{11}C]-glutamine may serve as a metabolic marker for probing glutamine-addicted tumors not detected by ^{18}F-FDG PET. The development of a convenient synthesis of L-[5-^{11}C]-glutamine as an alternative metabolic biomarker provides an exciting opportunity for advancing diagnosis and treatment of tumor. This novel tumor metabolic imaging agent may lead to new methods to appraise the metabolic status of tumor growth in human cancer by PET.

DISCLOSURE STATEMENT

The costs of publication of this article were defrayed in part by the payment of page charges. Therefore, and solely to indicate this fact, this article is hereby marked "advertisement" in accordance with 18 USC section 1734.

ACKNOWLEDGMENTS

We thank Drs. George Belka, Rajesh Kamble, and Richard Freifelder for providing excellent technical assistance. This work was supported in part by grants from Stand-Up 2 Cancer (SU2C) and the Cancer Research Institute and a Medical Scientist Training grant. No other potential conflict of interest relevant to this article was reported.

REFERENCES

1. Dang C. Rethinking the Warburg effect with myc micromanaging glutamine metabolism. *Cancer Res.* 2010;70:859–862.
2. Vander Heiden M, Locasale J, Swanson K, et al. Evidence for an alternative glycolytic pathway in rapidly proliferating cells. *Science.* 2010;329:1492–1499.
3. Warburg O. On the origin of cancer cells. *Science.* 1956;123:309–314.
4. DeBerardinis R, Cheng T. Q's next: the diverse functions of glutamine in metabolism, cell biology and cancer. *Oncogene.* 2010;29:313–324.
5. Weinberg F, Chandel N. Mitochondrial metabolism and cancer. *Ann N Y Acad Sci.* 2009;1177:66–73.
6. Rajagopalan KN, Deberardinis RJ. Role of glutamine in cancer: therapeutic and imaging implications. *J Nucl Med.* 2011;52:1005–1008.
7. Thompson C. Metabolic enzymes as oncogenes or tumor suppressors. *N Engl J Med.* 2009;360:813–815.
8. Vander Heiden M, Cantley L, Thompson C. Understanding the Warburg effect: the metabolic requirements of cell proliferation. *Science.* 2009;324:1029–1033.
9. Gillies RJ, Robey I, Gatenby RA. Causes and consequences of increased glucose metabolism of cancers. *J Nucl Med.* 2008;49(suppl 2):24S–42S.
10. Gambhir SS. Molecular imaging of cancer: from molecules to humans—Introduction. *J Nucl Med.* 2008;49(suppl 2):1S–4S.

11. Robey IF, Stephen RM, Brown KS, Baggett BK, Gatenby RA, Gillies RJ. Regulation of the Warburg effect in early-passage breast cancer cells. *Neoplasia.* 2008;10:745–756.
12. Kvamme E, Svenneby G. Effect of anaerobiosis and addition of keto acids on glutamine utilization by Ehrlich ascites-tumor cells. *Biochim Biophys Acta.* 1960;42:187–188.
13. Wise D, DeBerardinis R, Mancuso A, et al. Myc regulates a transcriptional program that stimulates mitochondrial glutaminolysis and leads to glutamine addiction. *Proc Natl Acad Sci USA.* 2008;105:18782–18787.
14. Dang C, Le A, Gao P. Myc-induced cancer cell energy metabolism and therapeutic opportunities. *Clin Cancer Res.* 2009;15:6479–6483.
15. Gao P, Tchernyshyov I, Chang T, et al. C-myc suppression of mir-23a/b enhances mitochondrial glutaminase expression and glutamine metabolism. *Nature.* 2009;458:762–765.
16. Dang CV. Pkm2 tyrosine phosphorylation and glutamine metabolism signal a different view of the Warburg effect. *Sci Signal.* 2009;2:pe75.
17. Dang CV. Myc, micrornas and glutamine addiction in cancers. *Cell Cycle.* 2009;8:3243–3245.
18. Erickson J, Cerione R. Glutaminase: a hot spot for regulation of cancer cell metabolism? *Oncotarget.* 2010;1:734–740.
19. Wang JB, Erickson JW, Fuji R, et al. Targeting mitochondrial glutaminase activity inhibits oncogenic transformation. *Cancer Cell.* 2010;18:207–219.
20. Conlon KC, Bading JR, DiResta GR, Corbally MT, Gelbard AS, Brennan MF. Validation of transport measurements in skeletal muscle with N-13 amino acids using a rabbit isolated hindlimb model. *Life Sci.* 1989;44:847–859.
21. Qu W, Zha Z, Ploessl K, et al. Synthesis of optically pure 4-fluoro-glutamines as potential metabolic imaging agents for tumors. *J Am Chem Soc.* 2011;133:1122–1133.
22. Surti S, Karp JS, Perkins AE, et al. Imaging performance of A-PET: a small animal PET camera. *IEEE Trans Med Imaging.* 2005;24:844–852.
23. Iwata R, Ido T, Takahashi T, Nakanishi H, Iida S. Optimization of [^{11}C]HCN production and no-carrier-added [1-^{11}C]amino acid synthesis. *Int J Rad Appl Instrum [A].* 1987;38:97–102.
24. Moorthy JN, Singhal N. Facile and highly selective conversion of nitriles to amides via indirect acid-catalyzed hydration using TFA or AcOH-H_2SO_4. *J Org Chem.* 2005;70:1926–1929.
25. Antoni G, Omura H, Ikemoto M, Moulder R, Watanabe Y, Langstrom B. Enzyme catalyzed synthesis of l-[4-^{11}C]aspartate and l-[5-^{11}C]glutamate. *J Labelled Comp Radiopharm.* 2001;44:287–294.
26. Dang CV. Glutaminolysis: supplying carbon or nitrogen or both for cancer cells? *Cell Cycle.* 2010;9:3884–3886.
27. McGivan JD, Bungard CI. The transport of glutamine into mammalian cells. *Front Biosci.* 2007;12:874–882.
28. Plathow C, Weber WA. Tumor cell metabolism imaging. *J Nucl Med.* 2008;49 (suppl 2):43S–63S.
29. McConathy J, Goodman Mark M. Non-natural amino acids for tumor imaging using positron emission tomography and single photon emission computed tomography. *Cancer Metastasis Rev.* 2008;27:555–573.
30. Yu W, Williams L, Camp V, Olson J, Goodman M. Synthesis and biological evaluation of anti-1-amino-2-[^{18}F]fluoro-cyclobutyl-1-carboxylic acid (anti-2-[^{18}F]FACBC) in rat 9L gliosarcoma. *Bioorg Med Chem Lett.* 2010;20:2140–2143.
31. Yu W, Williams L, Camp V, Malveaux E, Olson J, Goodman M. Stereoselective synthesis and biological evaluation of syn-1-amino-3-[^{18}F]fluorocyclobutyl-1-carboxylic acid as a potential positron emission tomography brain tumor imaging agent. *Bioorg Med Chem.* 2009;17:1982–1990.
32. Nye JA, Jarkas N, Schuster DM, et al. Biodistribution and human dosimetry of enantiomer-1 of the synthetic leucine analog anti-1-amino-2-fluorocyclopentyl-1-carboxylic acid. *Nucl Med Biol.* 2011;38:1035–1041.
33. Schuster DM, Savir-Baruch B, Nieh PT, et al. Detection of recurrent prostate carcinoma with anti-1-amino-3-^{18}F-fluorocyclobutane-1-carboxylic acid PET/CT and ^{111}In-capromab pendetide SPECT/CT. *Radiology.* 2011;259:852–861.
34. Okudaira H, Shikano N, Nishii R, et al. Putative transport mechanism and intracellular fate of trans-1-amino-3-1^{18}F-fluorocyclobutanecarboxylic acid in human prostate cancer. *J Nucl Med.* 2011;52:822–829.
35. Langen KJ, Hamacher K, Weckesser M, et al. *O*-(2-[^{18}F]fluoroethyl)-l-tyrosine: uptake mechanisms and clinical applications. *Nucl Med Biol.* 2006;33:287–294.
36. Lieberman BP, Plossl K, Wang L, et al. PET of glutaminolysis in tumors by ^{18}F-(2S,4R) 4-fluoroglutamine. *J Nucl Med.* 2011;52:1947–1955.
37. Qu W, Zha Z, Lieberman BP, et al. Facile synthesis [5-^{13}C-4-$^{2}H_2$]-l-glutamine for hyperpolarized MRS imaging of cancer cell metabolism. *Acad Radiol.* 2011;18:932–939.